Specific Absorption Rate Distribution in a Full-Scale Model of Man at 350 MHz

ANDRZEJ KRASZEWSKI, MARIA A. STUCHLY, SENIOR MEMBER, IEEE, STANISLAW S. STUCHLY, SENIOR MEMBER, IEEE, GEORGE HARTSGROVE, AND DANIEL ADAMSKI

Abstract—**A computer-controlled scanning system and an implantable triaxial electric-field probe have been used to obtain maps of the specific absorption rate (SAR) in various cross sections of a full-scale model of man. The model was exposed to a 350-MHz plane wave that provided various orientations of the electric-field vector with respect to the body. The results obtained are in general agreement with previously published theoretical and experimental data. The SAR distributions in the torso and head were in relatively good agreement with cylindrical and spherical models, respectively. Enhanced absorption in the neck and the limbs, as previously found by the thermographic method, was observed. This study provides much more detailed information than previously available, with an absolute accuracy of ±1 db.**

I. Introduction

THE AVERAGE specific absorption rate (SAR) has been extensively used in quantifying interactions of electromagnetic fields in the radio and microwave frequency range with biological systems. The importance of the distribution of SAR's within the exposed system is well recognized as an essential factor in quantifying biological effects. In recent years, numerous theoretical methods have been developed for dosimetry, as reviewed elsewhere [1]–[3]. Analyses of the so-called block model of man appear to be most promising in providing the SAR distribution [4]–[7]. Results of such analyses have recently been also utilized in calculating the thermal response of a man exposed to radio waves [8].

In view of the importance of SAR distribution, it is essential that theoretical data are quantitatively verified experimentally. Furthermore, as the capabilities of analytical methods are limited in treating such complex structures as biological bodies, experimental methods may offer the only viable means for studying the SAR distribution in models closely resembling the actual bodies under more complex exposure conditions (e.g., near-field exposure). There are three viable techniques for measuring SAR distributions. A thermographic method has been developed and successfully applied on scaled-down models [9]–[11]. The main limitations of this technique are a limited spatial resolution due to the small size of the models and a difficulty in incorporating the anatomical structure into such a small model. Conversely, if a full-scale model of man is analyzed by thermography, very high intensities of the exposure field are required. These limitations have led to the use of two other dosimetric techniques on full-scale models of man.

A nonperturbing temperature probe has been used to measure the SAR in a limited number of locations in a full-scale model of man exposed at frequencies of 1.29 and 2 GHz [12], [13], and models of other primates. An implantable electric-field probe offers an alternative tool for measuring the SAR distribution and has several advantages. In addition to being particularly suitable for measurements in full-scale models, the measurements are not dependent on the thermal properties of the model material. Not only the SAR, but also the direction of the electric field can be determined. Measurements can be performed in very low exposure fields, which do not cause any increase in the model temperature. Furthermore, the data can be conveniently obtained for a very large number of locations when an automatic probe positioning system is used.

In this paper, SAR distributions in a full-scale model of man exposed to a plane-wave at 350 MHz are presented. The data were obtained using a calibrated implantable electric-field probe and a computer-controlled scanning system. The exposure frequency of 350 MHz was selected because of the reported head resonance at this frequency [7] and the availability of SAR data for the block model of man [14].

II. Experimental Arrangement

A general view of the experimental arrangement is shown in Fig. 1. The system—except for the computer, the generator, and monitoring equipment—was placed in an anechoic chamber. An exposure field was produced by a resonant slot above the ground plane, having gain of 4.87 at 350 MHz. The antenna was located below the phantom model as illustrated in Fig. 1 for the E orientation (i.e., the electric-field vector parallel to the long axis of the body), or at the side of the phantom for the k orientation (i.e., the wave propagation from head to toe, the propagation vector parallel to the long axis of the body).

The scanning system was composed of a mechanical structure for supporting and positioning the probe and a

Manuscript received October 12, 1983; revised March 9, 1984. This work was supported by the Office of Naval Research, (U.S.A.), the Department of Health and Welfare Canada, and the Natural Sciences and Engineering Research Council of Canada.

A. Kraszewski, S. S. Stuchly, G. Hartsgrove, and D. Adamski are with the Department of Electrical Engineering, University of Ottawa, Ottawa, Ontario, Canada K1N 6N5.

M. A. Stuchly is with the Radiation Protection Bureau, Health and Welfare Canada, Ottawa, Ontario, Canada K1A 0L2.

0018-9480/84/0800-0779$01.00 ©1984 IEEE

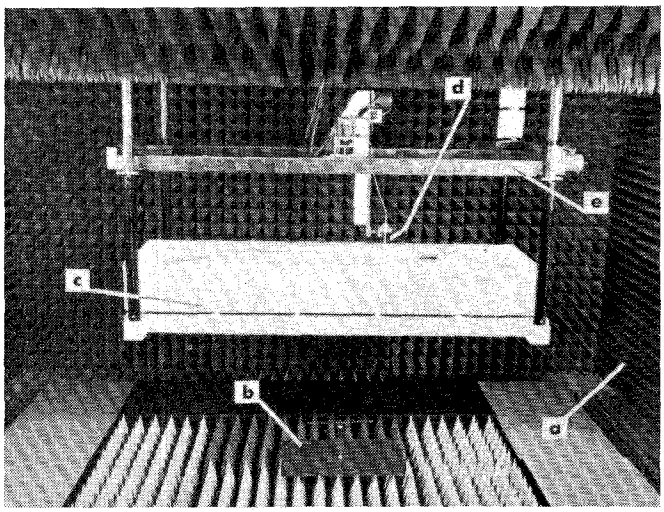

Fig. 1. Experimental arrangement (a) anechoic chamber, (b) antenna, (c) phantom model of the human body, (d) triaxial electric-field probe, and (e) mechanical structure for supporting and positioning the probe.

computer system for control of the experiment, data acquisition, storage, display, and recording. The probe could be placed at any location within a volume of $1.9\times 0.5\times 0.45$ m. The scanning resolution was 0.013 mm/step in each direction, and the position repeatability (uncertainty) was ± 0.05 mm. The probe could be moved at high speed with a velocity of approximately 12.5 mm/s, and at a low speed of 0.42 mm/s. The computer hardware and software are described elsewhere [15].

The full-scale plastic model shown in Fig. 2(a) had dimensions of a standard man. This plastic model was used to make a set of templates having exact dimensions of the plastic model in various cross sections (Figure 2(b)). These templates, in turn, were used to prepare 2.5-cm-thick styrofoam layers, which were glued together to obtain a hollow phantom of man (Fig. 2(c)). This phantom was filled with a mixture of water, sugar, and salt in such proportions that it had the following electrical properties: $\epsilon' = 38$ and $\sigma = 0.95$ S/m. These properties correspond to the tissue average properties at 350 MHz. The mixture had a relatively low viscosity, which facilitated penetration of the probe.

An implantable triaxial electric-field probe, model EIT 979,[1] was used to measure the electric-field intensity. This probe was previously fully characterized in terms of its sensitivity in tissue phantom material, noise, and modulation characteristics [16]. To improve the signal-to-noise ratio, and therefore the dynamic range of measurements, the radiofrequency signal was amplitude modulated at 516 Hz and a high-gain narrow-band amplifier was used at the output of the probe [16]. The probe sensitivity in the tissue phantom material was 2.1 $\mu V/(V^2/m^2)$, and the estimated calibration uncertainty was ± 1 dB. The minimum measurable electric-field intensity, with a signal-to-noise ratio of 10 and 1-Hz bandwidth amplifier, was 1.3 V/m (SAR = 1.6 mW/kg).

[1]Manufactured by Electronic Instrumentation and Technology Inc., Sterling, VA 22170, U.S.A.

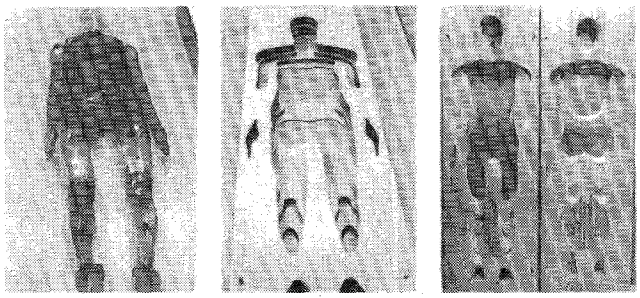

(a) (b) (c)

Fig. 2. Phantom model of man—design details, (a) plastic model of an average man, (b) set of templates, and (c) styrofoam mold.

III. Results and Discussion

The SAR values at several locations within the body in three cross sections separated by 5 cm are shown in Fig. 3. Each data point is an average of at least five (5) separate measurements performed on various days and with various incident power levels within the linear range of the system operation. Fig. 4 shows the same data along two selected axes, as indicated, in the cross section close to the body center. The bars indicate one standard deviation. In all experiments, the SAR values were normalized to an incident power density of 1 mW/cm^2 at a plane corresponding to the body surface or point closest to the radiation source. When these data are compared with experimental data available in the literature for scaled-down models at 450 MHz [11], it is seen that, despite the difference in the exposure frequency, there is good agreement. "Hot spots" in our measurements are found in the neck region, with the SAR values ranging from 86 to 196 mW/kg in the plane $z = 10$ cm (corresponding approximately to the body center). These data can be compared with a maximum of 120 mW/kg in the center cross section for exposure at 450 MHz [11]. Similarly, in the legs, the maximum SAR values are 110 and 147 mW/kg in our measurements and at 450 MHz [11], respectively. It appears that the location of the maximum SAR in the legs is somewhat different at the two frequencies. A hot spot, of somewhat smaller intensity than at 450 MHz [11], was observed by us in the arms. This may be due to a difference in the arms articulation in the two phantom models.

A general qualitative agreement can be observed between our data and the theoretical calculations for the block model [14]. However, there is a significant difference in the quantitative SAR distribution, the locations of the hot spots, and the maximum values of the SAR. The most likely explanation for the observed differences is that the shapes of the block model and our phantom are significantly different and the torso of the block model consisted of a relatively small number of cells. In particular, there are

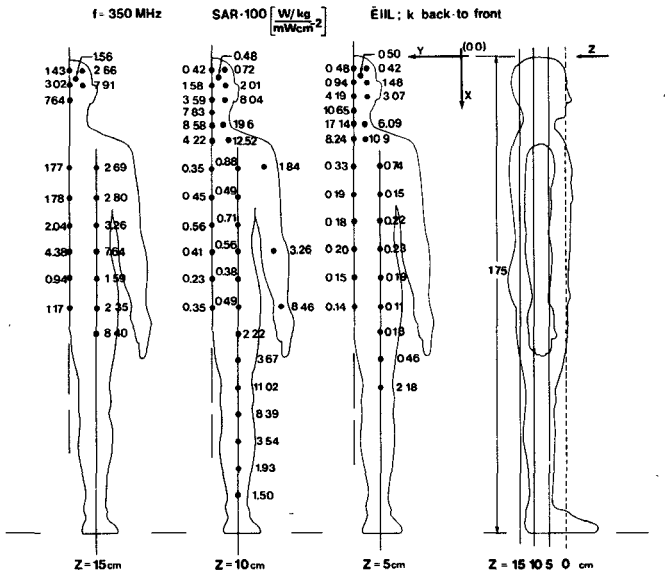

Fig. 3. Specific absorption rate (SAR) distribution (W/kg)*100 for a plane wave irradiation at a power density of 1 mW/cm^2 on the surface of the model, the electric field parallel to the long axis of the model $\bar{E} \parallel L$, the propagation k, from back to front, frequency 350 MHz.

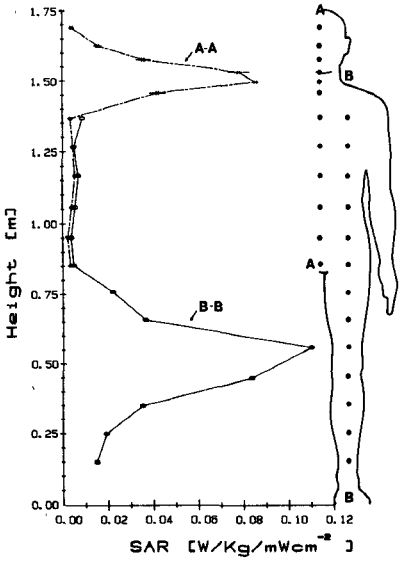

Fig. 4. Specific absorption rate (SAR) distribution along the man model height for two cross sections. 1 mW/cm^2 incident power density on the surface of the model, frequency 350 MHz $\bar{E} \parallel L$, k back to front, $z = 10$ cm (see Fig. 3, for z designation).

only two to three layers of cells in the block model, and our measurements indicate a rapid decrease of the SAR in the torso in the direction of the wave propagation (compare the SAR values at the same point for the three cross sections z in Fig. 3).

A rapid decrease in SAR values within the torso as a function of distance from the radiation source is further illustrated in Fig. 5. Since the SAR change is very rapid, values averaged over large size cells in the block model are obviously significantly different from those measured by the implantable probe, which provide averages for a rela-

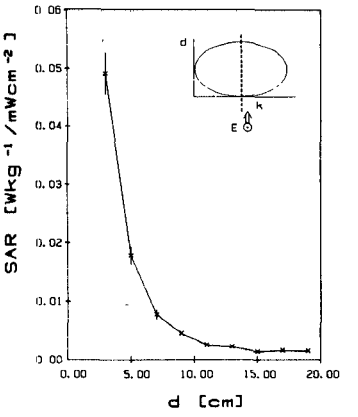

Fig. 5. Specific absorption rate (SAR) distribution in the upper torso (chest area −48 cm from the head top) along the axis as a function of the distance from the plane of the wave incidence: frequency 350 MHz, incident power density 1 mW/cm^2 in the plane tangent to the model $\bar{E} \parallel L$, k back to front.

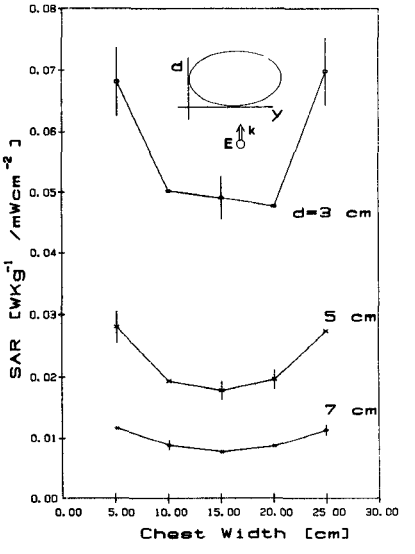

Fig. 6. Specific absorption rate (SAR) distribution in the upper torso (chest area—48 cm from the top of the head): frequency 350 MHz, incident power density 1 mW/cm^2 in the plane tangent to the model $\bar{E} \parallel L$, k back to front.

tively small volume. The deposition of energy at the body surface within the torso was also observed thermographically at 450 MHz [11].

A relatively good quantitative agreement between the calculated values for the block model [14] and our data was observed for the arms.

Fig. 6 shows the SAR distributions across the chest at various depths. Symmetry of the distribution within the uncertainty of measurements is observed for the center axis of the body. This is an expected result, confirming that measurements of the SAR within half of the body are sufficient.

The SAR distributions in the head of our model are shown in Fig. 7 for two orientations of the incident field with respect to the body. Corresponding calculated SAR distributions in a 16-cm-diameter sphere filled with the

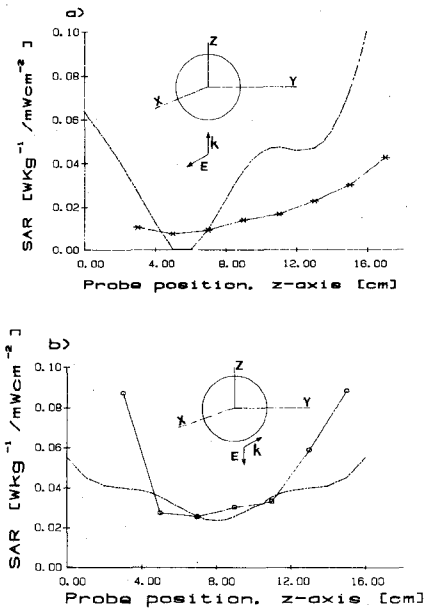

Fig. 7. Specific absorption rate (SAR) distribution in the head, frequency 350 MHz, incident power density 1 mW/cm^2, (a) $\bar{E} \parallel L$, (b) $k \parallel L$. The dashed lines show the calculated SAR in a 16-cm-diameter sphere.

same phantom material are also shown for comparison. It can be noted that the overall shape of the curves is similar; however, the quantitative results are not surprisingly different, in view of the actual shape of the head. The SAR distribution in the head appears to be significantly different than that for the block model of man [14]. However a detailed analysis, which is outside of the scope of this paper, would be necessary to compare the results.

IV. Conclusions

Measurements of the specific absorption rate (SAR) distribution for a full-scale model of man filled with a phantom material having average tissue permittivity were performed at 350 MHz for a far-field exposure. Use of a computer-controlled mechanical scanning system and an implantable isotropic electric-field probe provided a good spatial resolution, an excellent reproducibility of results of ± 0.5 dB, and a good absolute uncertainty of ± 1 dB. The measurements were fully automated and, after proper calibrations and preparation, a large number of data points were conveniently obtained.

At a frequency of 350 MHz, a generally nonresonant behavior of the human body with maximum energy absorption at the surface on which the radiation is incident was confirmed. This conclusion did not, however, apply to the head, neck, and the limbs, where more complex distributions of the SAR were observed.

Our experimental data were in good agreement with reported experimental results at 450 MHz obtained by the thermographic technique [11]; however, only a few features of the distribution could be compared.

General qualitative agreement with theoretical data for the block model of man [14] appears to exist; however, our data are significantly different, particularly in the head–neck region [7]. Most likely, the differences are due to differences in shapes of the models and a limited number of cells for the block model, particularly in terms of layers (2 layers [7]).

Acknowledgment

Numerical calculations and helpful discussions with Drs. O. P. Gandhi and I. Chatterjee from the University of Utah, Salt Lake City, and stimulating discussions with Dr. D. Hill from the Canadian Department of Defence are greatfully acknowledged.

References

[1] C. H. Durney, "Electromagnetic dosimetry for models of humans and animals: A review of theoretical and numerical techniques," *Proc. IEEE*, vol. 68, pp. 33–40, 1980.
[2] O. P. Gandhi, "State of knowledge for electromagnetic absorbed dose in man and animals," *Proc. IEEE*, vol. 68, pp. 24–32, 1980.
[3] M. A. Stuchly, "Dosimetry of radio frequency and microwave radiation: Theoretical analyses," in *Biological Effects and Dosimetry of Nonionizing Radiation*, M. Grandolfo, S. M. Michaelson, Eds. New York: Plenum Publishing, 1983, pp. 163–177.
[4] K. M. Chen and B. S. Guru, "Induced EM fields inside human bodies irradiated by EM waves up to 500 MHz," *J. Microwave Power*, vol. 12, pp. 173–183, 1977.
[5] ——, "Internal EM fields and absorbed power density in human torso induced by 1–500 MHz EM waves," *IEEE Trans. Microwave Theory Tech.*, vol. MTT-25, pp. 746–756, 1977.
[6] M. J. Hagmann, O. P. Gandhi, and C. M. Durney, "Numerical calculation of electromagnetic energy deposition for a realistic model of man," *IEEE Trans. Microwave Theory Tech.*, vol. MTT-27, pp. 804–809, 1979.
[7] M. J. Hagmann, O. P. Gandhi, J. A. D'Andrea, and I. Chatterjee, "Head resonance: Numerical solutions and experimental results," *IEEE Trans. Microwave Theory Tech.*, vol. MTT-27, pp. 809–813, 1979.
[8] R. J. Spiegel, "The thermal response of a human in the near-zone of a resonant thin-wire antenna," *IEEE Trans. Microwave Theory Tech.*, vol. MTT-30, pp. 177–185, 1982.
[9] A. W. Guy, "Analysis of electromagnetic fields induced in biological tissues by thermographic studies in equivalent phantom models," *IEEE Trans. Microwave Theory Tech.*, vol. MTT-19, pp. 205–214, 1971.
[10] A. W. Guy, M. D. Webb, and C. C. Sorensen, "Determination of power absorption in man exposed to high frequency electromagnetic fields by thermographic measurements on real models," *IEEE Trans. Biomed. Eng.*, vol. BME-23, pp. 361–371, 1976.
[11] A. W. Guy, "Non-ionizing radiation: Dosimetry and interaction," in *Proc. ACGIH Topical Symp.*, Nov. 26–28, 1979, pp. 75–101.
[12] R. G. Olsen, "Preliminary studies: Far-field microwave dosimetric measurements of a full-scale model of man," *J. Microwave Power*, vol. 14, pp. 383–388, 1979.
[13] ——, "Far-field dosimetric measurements in a full-sized man model at 2.0 GHz," *Bioelectromagn.*, vol. 3, pp. 433–441, 1982.
[14] O. P. Gandhi and I. Chatterjee, private communication, 1983.
[15] S. S. Stuchly, M. Barski, B. Tam, G. Hartsgrove, and S. Symons, "Computer-based scanning system for electromagnetic dosimetry," *Rev. Sci. Instrum.*, vol. 54, no. 11, pp. 1547–1550, 1983.
[16] M. A. Stuchly, A. Kraszewski, and S. S. Stuchly, "Implantable electric field probes—Some performance characteristics," *IEEE Trans. Biomed. Eng.*, vol. BME-31, 1984, pp. 526–531, July 1984.

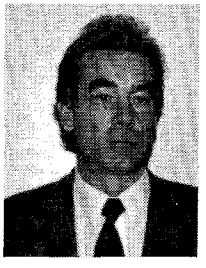

Andrzej Kraszewski was born in Poznań, Poland, on April 22, 1933. He received the M.Sc. degree in electrical engineering from the Technical University of Warsaw, Warsaw, Poland, in 1958, and the D.Sc. degree in technical sciences from the Polish Academy of Sciences, (PAN), Warsaw, in 1973.

Beginning in 1953, he was employed at the Telecommunication Institute, Warsaw, in the research and development of microwave components and systems. Beginning in 1963, he joined

UNIPAN Scientific Instruments, a subsidiary of the Polish Academy of Sciences, as the Head of the Microwave Laboratory. Starting in 1972, he was Manager of the Microwave Department of WILMER Instruments and Measurements, a subsidiary of the Polish Academy of Sciences in Warsaw, where he co-developed microwave instruments for moisture-content measurements and control. Since November 1980, as a Visiting Professor at the University of Ottawa, Canada, he has been engaged in research of interactions between dielectrics and electromagnetic fields. He is the author of several books on microwave theory and techniques, has published more than 80 technical papers on the subject, and holds 18 patents. He received several professional awards, among them the State Prize in Science in 1980.

Dr. Kraszewski is a member of the International Microwave Power Institute, the Polish Electricians Association, and is a member of the Editorial Board of the *Journal of Microwave Power*.

Maria A. Stuchly (M'71–SM'76) received the M.S. and Ph.D. degrees in electrical engineering from Warsaw Technical University and Polish Academy of Sciences in 1962 and 1970, respectively.

From 1962 to 1970, she was employed as a Senior R & D Engineer in a subsidiary of the Polish Academy of Sciences, in Warsaw, Poland. Between 1970 and 1976, she was engaged in research in the field of microwave instrumentation and measurements, and microwave power applications at the Departments of Electrical Engineering and Food Science at the University of Manitoba. Since 1976, she has been with the Non-Ionizing Radiation Section, Radiation Protection Bureau, Health and Welfare Canada, where she is responsible for the development of microwave radiation protection standards and carries out research in the field of biological effects of microwave radiation. She is also nonresident Professor of electrical engineering at the University of Ottawa.

Dr. Stuchly is a member of the Board of Directors of the Bioelectromagnetics Society and a member of the IEEE Technical Committee of Man and Radiation.

Stanislaw S. Stuchly (M'70–SM'72) was born in Lwow, Poland on November 20, 1931. He received the B.Sc. degree from the Technical University, Gliwice, Poland, and the M.Sc. degree from the Warsaw Technical University, both in electrical engineering, in 1953 and 1958, respectively, and the Ph.D. degree from the Polish Academy of Sciences, Warsaw, Poland in 1968.

From 1953 to 1959, he was a Research Engineer in the Industrial Institute for Telecommunications, Warsaw, Poland. From 1959 to 1963, he was with the Warsaw Technical University. In 1963, he joined UNIPAN—Scientific Instruments, subsidiary of the Polish Academy of Sciences. From 1970 to 1976, he was with the University of Manitoba, Winnipeg, Canada. Since 1977, he has been with the University of Ottawa, Canada, where he is presently a Professor of electrical engineering.

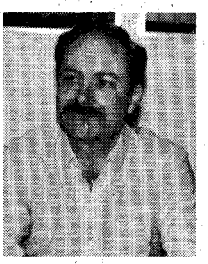

George Hartsgrove was born in Brantford, Ontario, Canada, on March 28, 1949. He graduated from Mohawk College, Hamilton, Ontario, in 1970.

Since 1976, he has been involved in bioelectromagnetic research at the National Research Council and, since 1981, at the University of Ottawa, Department of Electrical Engineering.

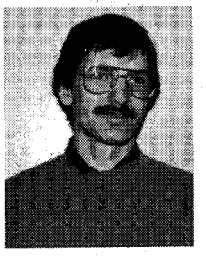

Daniel Adamski was born in Sudbury, Ontario, Canada, on November 22, 1960. He received the B.A.Sc. degree in electrical engineering from the University of Ottawa, Ontario, Canada.

From 1982–1983, he was a Research Engineer with the University of Ottawa, where he participated in the implementation of a dosimetry laboratory. He is currently pursuing the M.A.Sc. degree in Electrical Engineering at the University of Ottawa.